



Discover Generics

Cost-Effective CT & MRI Contrast Agents



WATCH VIDEO

AJNR

The nuclear trail sign in thoracic herniated disks.

E E Awwad, D S Martin and K R Smith, Jr

AJNR Am J Neuroradiol 1992, 13 (1) 137-143
<http://www.ajnr.org/content/13/1/137>

This information is current as
of June 23, 2025.

The Nuclear Trail Sign in Thoracic Herniated Disks

Eric E. Awwad,¹ David S. Martin,¹ and Kenneth R. Smith, Jr.²

Purpose and Methods: Postmyelography CT studies of 84 patients with 114 thoracic herniated disks were reviewed for endplate irregularity, sclerosis, and/or disk-space calcification that could suggest a migratory path of the herniated fragment. **Results:** Abnormal straight or curvilinear densities (the "nuclear trail sign") were present at the level of the disk or endplate in 46% of the cases. MR studies of 35 thoracic herniated disks were also examined. Similar changes were likewise present in 44%. **Conclusion:** The frequent occurrence of this finding in the mid and lower thoracic spine renders it a useful secondary sign for thoracic herniated disks, although false positives do occur.

Index terms: Spine, intervertebral disk herniation; Myelography; Spine, computed tomography; Spine, magnetic resonance

AJNR 13:137-143, January/February 1992

Herniation of the nucleus pulposis is caused by a combination of biomechanical factors, chronic degenerative structural changes, and superimposed mechanical forces. These factors can induce endplate herniation and disk-space calcification in a peculiar spatial orientation suggestive of the migratory path of the herniated nuclear fragment.

Postmyelography computed tomography (CT) studies were examined for such changes to determine the frequency of these findings at thoracic interspaces with nuclear herniation. The imaging characteristics with postmyelography CT and magnetic resonance imaging (MR) were also noted.

Subjects and Methods

Postmyelographic CT studies of 114 thoracic herniated disks in 84 patients were retrospectively reviewed. Three millimeter axial scans were routinely obtained with the gantry angled parallel to the disk space following iopamidol myelography. Occasionally only 5-mm, 4-mm or 1.5-mm scans were available. Wide and narrow window widths were

available for evaluation. The postmyelography CT studies were reviewed for endplate irregularity consistent with endplate herniation that extended from the center of the endplate in the axial plane to the protruded fragment. Strands of endplate sclerosis or disk-space calcification that extended in a similar pattern were also noted. Only findings that were observed by both of the reviewing neuroradiologists were included.

MR images of 35 thoracic herniated disks in 22 patients were also reviewed. Sagittal and axial images were available in all; however, multiple pulsing sequences and imaging parameters were utilized. Sagittal T1-weighted images were available in all but one instance. Sagittal T2*-weighted images were available in approximately two-thirds, while intermediate and T2-weighted images were available in most of the remainder. Axial T1-weighted images were available in 21, axial T2*-weighted images were available in 23, and axial T2-weighted images were available in one instance. Twenty-one of these disks were also evaluated by CT, 17 of which were included in the postmyelography CT study. Eight of the MR studies were obtained solely because a trail was detected by postmyelography CT and were consequently excluded from the MR frequency analysis.

Results

Forty-six percent (53/114) of thoracic herniated disks evaluated by postmyelography CT demonstrated abnormal straight or curvilinear densities located at the level of the disk or at the endplate. In the axial plane, they originated well within the center of the disk space or vertebral body endplate and extended to the protruded fragment. Seventy-nine percent (42/53) with the

Received March 11, 1991; revision requested May 9; revision received September 10; final acceptance September 19.

¹ Department of Radiology, St. Louis University Medical Center, 3635 Vista at Grand, P.O. Box 15250, St. Louis, MO 63110-0250. Address reprint requests to E. E. Awwad.

² Division of Neurosurgery, St. Louis University Medical Center, St. Louis, MO 63110-0250.

AJNR 13:137-143, Jan/Feb 1992 0195-6108/92/1301-0137

© American Society of Neuroradiology

Fig. 1. A, Right parasagittal herniated disk at the T7/T8 level with disk density protruding into the superior end plate forming a path from the center of the disk to the protruded fragment. There is diffuse increased density of the disk material in the pathway consistent with slight calcification of the disk. The end plate wall of the herniation (*arrows*) demonstrates no sclerotic margin.

B, At a slightly more cephalad level portions of the end plate are better demonstrated forming a thin sclerotic margin (*arrows*).

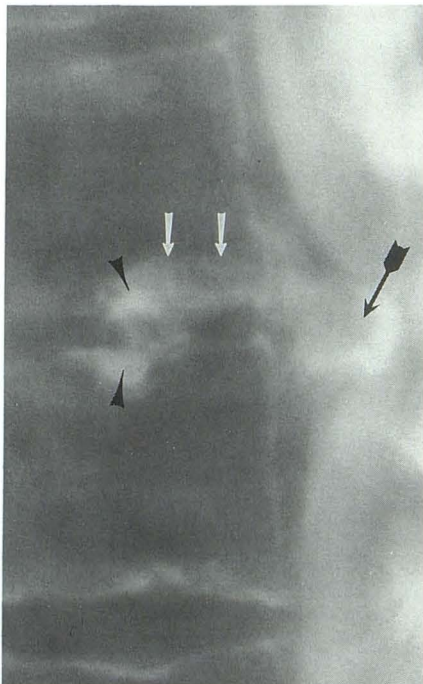
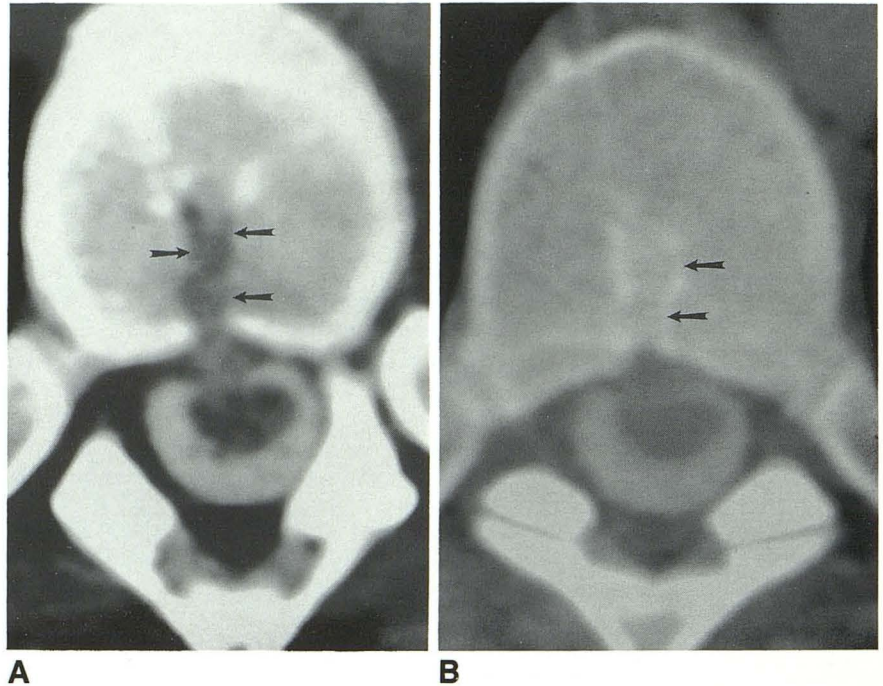


Fig. 2. Sagittal tomogram with intrathecal contrast at T7/T8 demonstrates a calcified nucleus pulposus (*arrowheads*), calcified disk fragment (*large arrow*), and end plate herniation (*white arrows*) extending from the nucleus pulposus to the spinal canal. Surgically confirmed herniation.

sign demonstrated disk density within bone compatible with endplate herniation (Fig. 1). This resulted in an enlarged tunnel extending from the nucleus pulposus to the intraspinal herniation

(Fig. 2). The thickness of the reflected endplate forming the wall of the herniation was variable. It could be barely perceptible (Fig. 1A), thin (Fig. 1B), or relatively thick (Fig. 3). The width of the defect ranged from moderately wide (Fig. 1) to narrow (Fig. 4). Twenty-one percent (11/53) demonstrated only a hyperdense trail (Fig. 5), presumably representing endplate sclerosis about similar endplate herniation in which the invagination was not readily appreciated on the axial scans. Thirty-eight percent (16/42) of those with definite endplate herniation also demonstrated endplate sclerosis. Occasionally, it was difficult to identify whether the increased attenuation near the invaginated endplate was endplate sclerosis or adjacent disk calcification. Some trail signs were primarily due to disk calcification (Fig. 6) or contained disk calcification (Fig. 1A).

The nuclear trail sign was seen in 52% (50/96) of disks when the disks were at the T6/T7 level or below. Only 17% (3/18) or the thoracic herniated disks detected above this level demonstrated the sign (Table 1).

In one patient, a defect was suspected at T4/T5 on the myelogram. Postmyelographic CT at the level of the disk demonstrated no herniation but the presence of a trail sign was noted (Fig. 4). By extending the number of slices to cover more of the vertebral body, a free fragment was identified in a more cephalad location. We have, however, detected several similar trails that did

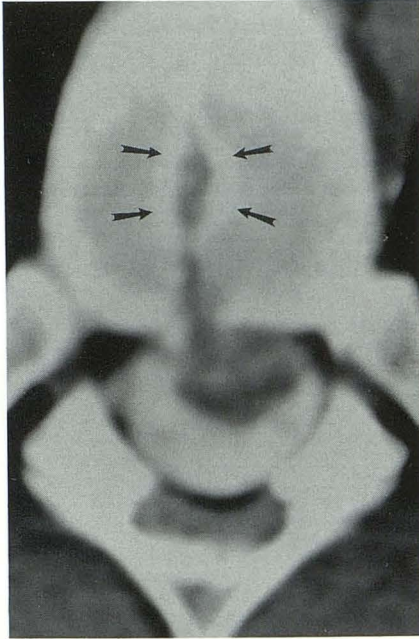


Fig. 3. T6/T7 herniated disk with obvious invagination into the endplate. The wall of the proximal portion of the trail (*arrows*) is thick most likely representing sclerosis about the end plate.

not completely extend to the disk margin or demonstrate intraspinal herniation (Fig. 7).

A trail sign was demonstrated in 12 of the 27 thoracic herniated disks randomly evaluated by MR imaging (Table 2) and in all eight scanned solely because a trail was detected by postmyelography CT. Some generalized observations are:

1. Endplate herniation was generally best demonstrated on axial T2*-weighted images. The disk demonstrated increased signal intensity in stark contrast to the low signal intensity of the bone (Figs. 8 and 9).

2. The trail was less often demonstrated on axial T1-weighted sequences, probably due to a lack of contrast between the disk and the bone marrow and the gap that was frequently present between slices (Figs. 10 and 11).

3. Axial intermediate and T2-weighted images were less satisfactory because only portions of the disk (and endplate herniation) had sufficient T2 prolongation to provide contrast with the dark bone.

4. Although sagittal images were useful in demonstrating the posterior herniation, and occasionally demonstrated some degree of endplate herniation, the continuity of the endplate herniation with the posterior herniation was not readily visible.

5. In the several instances where postmyelography CT and MR images were compared, the trail sign was generally more conspicuous on postmyelography CT.

6. In three cases where the postmyelography CT trail demonstrated linear endplate sclerosis without obvious endplate herniation, MR images were obtained. The trail was evident as decreased signal on T1 and T2* axial images in one instance, was of decreased signal on T1 and not present

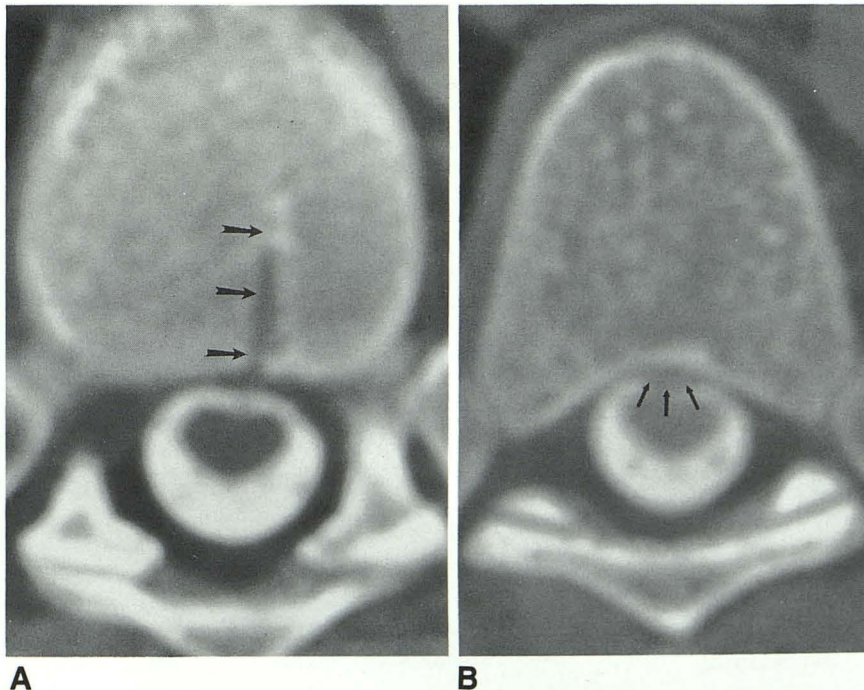


Fig. 4. A, Superior endplate herniation at T4/T5 forming a trail (*arrows*) to the posterior aspect of the disk without abnormal disk protrusion.

B, A small free fragment (*arrows*) was detected at a more cephalad level with spinal cord deformation.

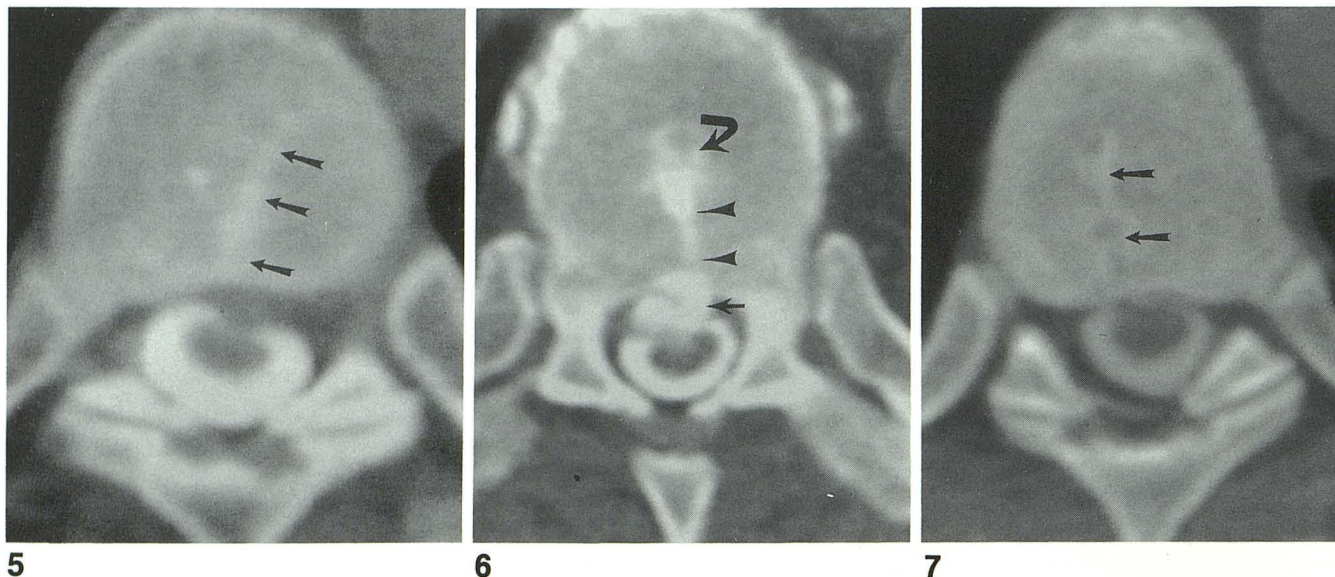
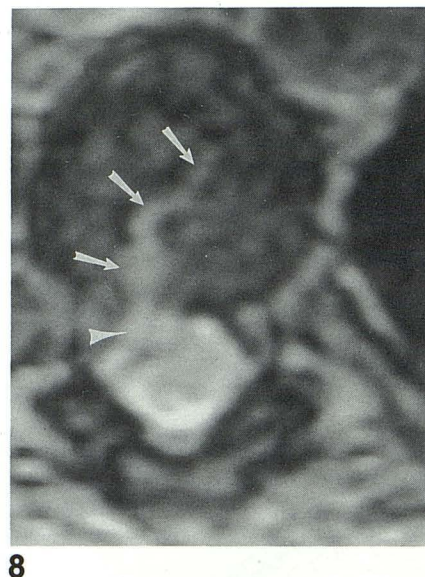


Fig. 5. Left parasagittal herniated disk at T7/T8 with a hyperdense trail (arrows) extending from the left lateral aspect of the center of the disk to the protruded fragment. This probably represents focal endplate sclerosis. The herniation was surgically confirmed.

Fig. 6. Large calcified thoracic herniated disk at T7/T8. There is calcification of the nucleus pulposus (curved arrow), the herniated fragment (arrow), and the disk material in between (arrowheads). Surgically confirmed herniation.

Fig. 7. Linear endplate herniation (arrows) at T7/T8 without evidence of posteriorly herniated disk.

Fig. 8. Axial MR image (1.5 T multi-planar gradient recalled (MPGR)/30° TR/TE 714/15/4) at T6/T7 with a prominent hyperintense trail (arrows) and posterior herniation (arrowhead). (Reprinted courtesy of Thomas Noland and Terry Weaver, Mid-County MRI, St. Louis, MO).



on T2* images in another (Fig. 12), and was present as increased signal on the T2* images in the third. The latter case was felt to better reflect the endplate herniation not appreciated on post-myelography CT.

Discussion

We have described a subset of cartilaginous (Schmorl's) nodes characterized by a linear or curvilinear pattern that can be contiguous with a posteriorly herniated thoracic disk. There are a number of possible explanations for the nuclear trail sign.

First, we consider it most likely that the endplate and posterior herniation occur simultaneously due to a unique combination of forces that

may occur with occult or obvious trauma. Under high vertical loads, disks tend to herniate superiorly and inferiorly into the endplates, while torsion and flexion tend to damage the annulus resulting in posterior and posterolateral herniations (1-3).

Alternatively, synchronous degenerative phenomena may occur. During disk degeneration a variety of biochemical and structural changes take place. Concentric and radially oriented fissures arise due to initial annular degeneration, which accelerate further changes. Nuclear and annular tissue may prolapse through these annular rents (1, 4). Adjacent degeneration of the cartilaginous endplates contributes to intraosseous disk displacement (5). Thus, we would be observing a chronic degenerative process with

TABLE 1: Postmyelography CT of thoracic HNPs^a

	Disk Space Level												Total
	T1	T2	T3	T4	T5	T6	T7	T8	T9	T10	T11	T12	
Number of HNPs	2	2	4	3	7	19	29	18	11	5	8	6	114
Number of HNPs with sign			1	1	1	10	18	7	7	2	4	2	53
Endplate herniation				1	1	4	7	3	5	1	2	2	26
Endplate sclerosis			1			3	4	1	1		1		11
Endplate herniation and sclerosis						3	7	3	1	1	1		16
Calcified disk path						1	4					1	6

^a HNPs, herniated disks.

TABLE 2: MR of thoracic HNPs^a

	Disk Space Level												Total
	T1	T2	T3	T4	T5	T6	T7	T8	T9	T10	T11	T12	
Number of HNPs			1	1	4	2	6	4	1	1	7		27
Number of HNPs with sign					2	2	4	1	1		2		12

^a HNPs, herniated disks.

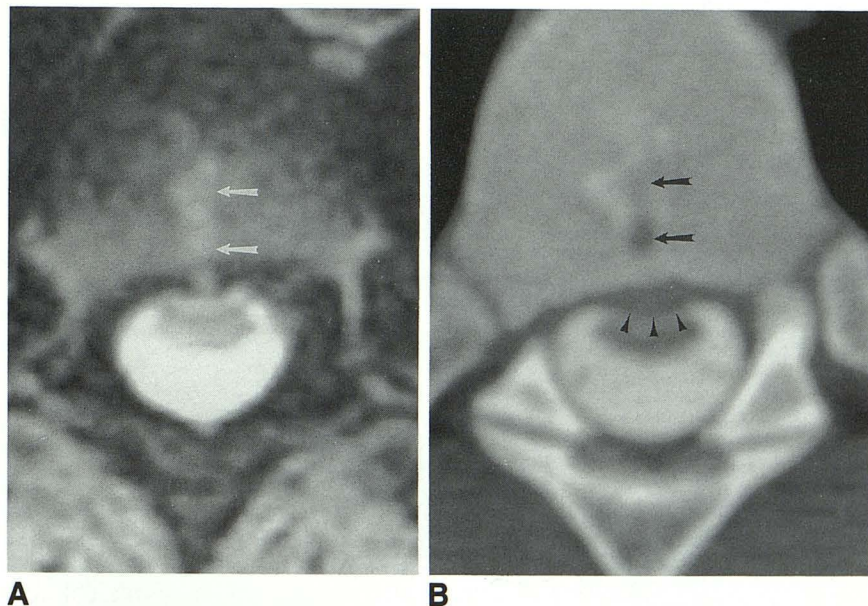


Fig. 9. A, Axial MR image (1.5 T MPGR/30° TR/TE 1000/15/2) at T6/T7 demonstrating a hyperintense trail (arrows).

B, CT myelogram at the inferior aspect of T6 demonstrating corresponding cephalad endplate herniation (arrows) and posterior herniation (arrowheads) deforming the spinal cord. The endplate defect continued to the spinal canal on an adjacent scan.

simultaneous superoinferior and posterior migration.

A cause and effect relationship should also be considered. Schmorl's nodes, when linear, may help direct the path of subsequent disk herniation. Such a tunnel may mechanically facilitate posterior migration of nuclear material. Also, alterations in the endplate cartilage or subchondral bone at such cartilaginous nodes could interfere with the nutrient supply of the disk from the vertebral body (6). This would conceivably create a weak point within the disk through which sub-

sequent nuclear material may travel. On the other hand, damage to the endplates occurring during posterior disk herniation could create focal weak spots through which subsequent intraosseous herniation occurs. Regardless of the initial events, repair and further degeneration of the disks, along with occasional calcification, take place along this path.

We have yet to see this sign in the cervical or lumbar region. Since the effect is noted particularly in the mid and lower thoracic regions, it is plausible that the unique combination of force

Fig. 10. A, Axial T1-weighted image (1.5 T spin echo TR/TE 600/20/4) at the T8/T9 level. A large calcified thoracic herniated disk(*) is present within the spinal canal. A path of low signal intensity through the adjacent endplate (arrows) forms the trail.

B, Sagittal intermediate weighted image (1765/30/2) with signal void due to calcified herniated disk fragment (arrow).

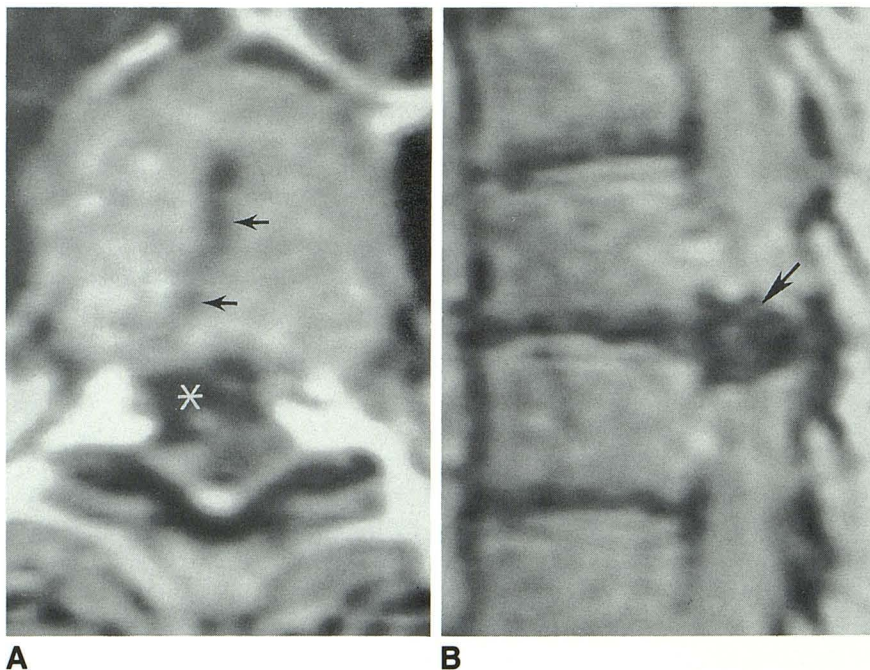
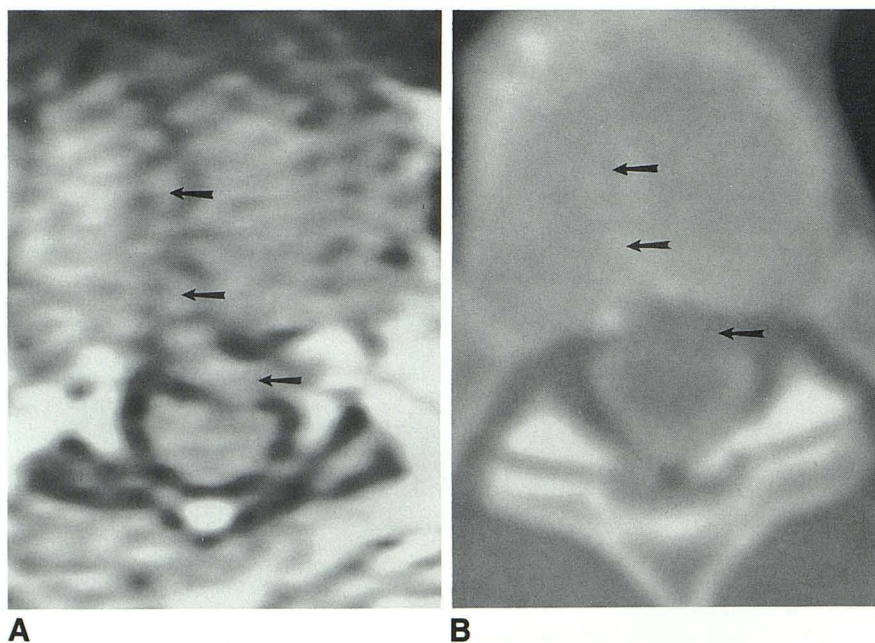


Fig. 11. A, Axial T1-weighted image (1.5 T spin echo TR/TE 600/11/2) at T7/8. The endplate and posterior herniations (arrows) are isointense with the bone marrow, accentuated by the signal void from the endplate.

B, Corresponding CT myelogram with herniations (arrows).



vectors necessary to produce this sign operates there. If the endplate herniation does occur initially, the distribution would be explained by a theoretical regional predisposition for such focal weak areas of the cartilaginous endplates that evolve into this particularly oriented subset of Schmorl's nodes. Conversely, the endplates in the region may be more prone to injury during posterior herniation.

While reviewing the literature, we found multiple illustrations of this sign with CT, including pathway calcification (7-11) and endplate herniation (12, 13). We also discovered examples of this appearance in the MR literature. Axial T1- (11, 14) and T2*- (15) weighted images demonstrated endplate herniation forming a trail.

In conclusion, we have described a radiographic sign that was present in approximately

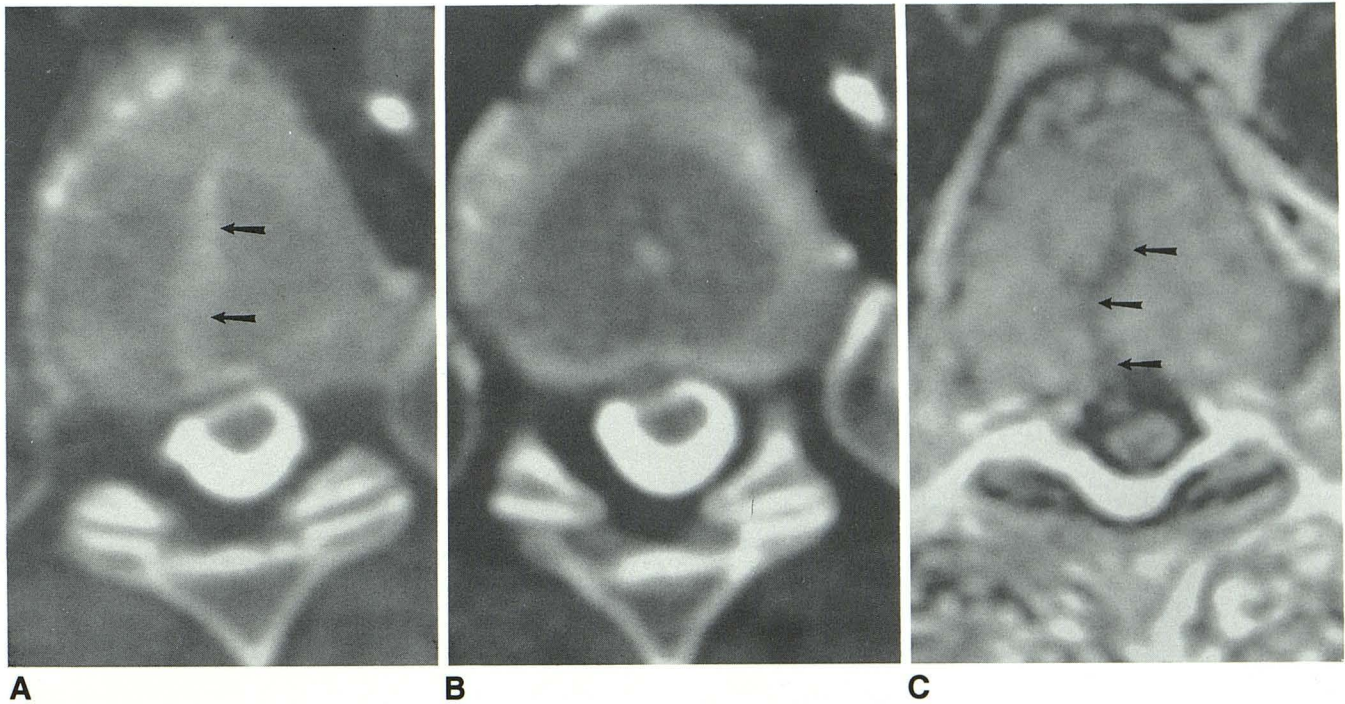


Fig. 12. A, Endplate sclerosis (arrows) at T6/T7 forming a trail. No endplate herniation was evident. B, At the level of the interspace, the posterior herniation is more evident. C, Corresponding axial T1-weighted image (1.5 T spin echo TR/TE 600/16/1) with trail (arrows).

one-half of the thoracic herniated disks evaluated. We suggest that it describes the path of herniation of the nuclear fragment. It seems probable that the endplate herniation and posterior herniation occur simultaneously, although we have no convincing evidence that one does not precede the other. The presence of well-defined sclerosis and dystrophic calcification in many of these instances suggest that many of these disk herniations are chronic at the time of detection. In addition to raising possibilities as to the etiology of thoracic nuclear herniation, the trail sign occurs frequently enough to provide a secondary sign of thoracic herniated disks, although false positives do occur.

References

1. Modic MT. Degenerative disorders of the spine. In: Modic MT, Masaryk TJ, Ross JS, eds. *Magnetic resonance imaging of the spine*. Chicago: Year Book Medical Publishers, 1989:75-119
2. Roaf R. A study of the mechanics of spinal injuries. *J Bone Joint Surg (Br)* 1960;42:810-823
3. Brown T, Hansen RJ, Yorra AJ. Some mechanical tests on the lumbosacral spine with particular reference to the intervertebral discs: a preliminary report. *J Bone Joint Surg (Am)* 1957;39:1135-1164
4. Lindblom BK, Hultqvist G. Absorption of protruded disc tissue. *J Bone Joint Surg (Am)* 1950;32:557-560
5. Resnick D, Niwayama G. Intravertebral disk herniations: cartilaginous (Schmorl's) nodes. *Radiology* 1978;126:57-65
6. Resnick D, Niwayama G. Major types of degenerative diseases of the spine. In: Resnick D, Niwayama G, eds. *Diagnosis of bone and joint disorders*. 2nd ed. Philadelphia: W.B. Saunders Company, 1988:1482-1489
7. Ryan RW, Lally JF, Kozic Z. Asymptomatic calcified herniated thoracic disks: CT recognition. *AJNR* 1988;9:364-365
8. Benjamin V. Diagnosis and management of thoracic disc disease. In: Weiss MH, ed. *Clinical neurosurgery*. Baltimore: Williams & Wilkins, 1983;30:581, 584
9. van Duym FC van A, van Wiechen PJ. Herniation of calcified nucleus pulposus in the thoracic spine. *J Comput Assist Tomogr* 1983;7:1123
10. Bury RW, Powell T. Prolapsed thoracic intervertebral disc: the importance of CT assisted myelography. *Clin Radiol* 1989;40:417
11. Francavilla TL, Powers A, Dina T, Hugo V. MR imaging of thoracic disk herniations. *J Comput Assist Tomogr* 1987;11:1063-1064
12. Bhole R, Gilmer RE. Two-level thoracic disc herniation. *Clin Orthop* 1984;190:130
13. Alvarez O, Roque CT Pampati M. Multilevel thoracic disk herniations: CT and MR studies. *J Comput Assist Tomogr* 1988;12:650
14. Enzmann DR. Degenerative disc disease. In: Enzmann DR, DeLaPaz RL, Rubin JB, eds. *Magnetic resonance of the spine*. The C.V. Mosby Company, 1990;10:462
15. Enzmann DR, Griffin C, Rubin JB. Potential false-negative MR images of the thoracic spine in disk disease with switching of phase- and frequency-encoding gradients. *Radiology* 1987;165:637